Effects of high energy Au-ion irradiation on the microstructure of diamond films

Shih-Show Chen, Huang-Chin Chen, Wei-Cheng Wang, Chi-Young Lee, I-Nan Lin, Jinghua Guo, and Ching-Lin Chang

Citation: Journal of Applied Physics **113**, 113704 (2013); doi: 10.1063/1.4795507
View online: http://dx.doi.org/10.1063/1.4795507
View Table of Contents: http://scitation.aip.org/content/aip/journal/jap/113/11?ver=pdfcov
Published by the AIP Publishing

Effects of high energy Au-ion irradiation on the microstructure of diamond films

Shih-Show Chen,[1,2] Huang-Chin Chen,[1,3] Wei-Cheng Wang,[1] Chi-Young Lee,[3] I-Nan Lin,[1] Jinghua Guo,[4] and Ching-Lin Chang[1,a)]
[1]*Department of Physics, Tamkang University, Tamsui, New-Taipei 251, Taiwan*
[2]*Department of Information Technology and Mobile Communication, Taipei College of Maritime Technology, Tamsui, New-Taipei 251, Taiwan*
[3]*Department of Materials Science and Engineering, National Tsing Hua University, Hsinchu 300, Taiwan*
[4]*Advanced Light Source, Lawrence Berkeley National Laboratory, Berkeley, California 94720, USA*

(Received 5 November 2012; accepted 2 March 2013; published online 18 March 2013)

The effects of 2.245 GeV Au-ion irradiation and subsequent annealing processes on the evolution of microstructure of diamond films with microcrystalline (MCD) or ultra-nanocrystalline (UNCD) granular structure were investigated, using near edge x-ray absorption fine structure and electron energy loss spectroscopy in transmission electron microscopy. For MCD films, the Au-ion irradiation disintegrated some of the diamond grains, resulting in the formation of nano-sized carbon clusters embedded in a matrix of amorphous carbon (a-C). The annealing process recrystallized the diamond grains and converted the a-C into nano-sized graphite particulates and, at the same time, induced the formation of nano-sized *i-carbon* clusters, the bcc structured carbon with $a_0 = 0.432$ nm. In contrast, for UNCD films, the Au-ion irradiation transformed the grain boundary phase into nano-sized graphite, but insignificantly altered the crystallinity of the grains of the UNCD films. The annealing process recrystallized the materials. In some of the regions, the residual a-C phases were transformed into nano-sized graphites, whereas in other regions *i-carbon* nanoclusters were formed. The difference in irradiation-induced microstructural transformation behavior between the MCD and the UNCD films is ascribed to the different granular structures of the two types of films. © *2013 American Institute of Physics*. [http://dx.doi.org/10.1063/1.4795507]

I. INTRODUCTION

Diamond exhibits several superior properties in comparison to other semi-conducting materials, such as the wide band gap, high electron hole pair mobility, short carrier lifetime, and extreme resilience to harsh environments. Diamond films have been extensively investigated for the application as radiation detectors.[1–4] During the growth of microcrystalline diamond (MCD) films, hydrogen is usually incorporated into the materials and is presumed to reside at the grain boundaries. Studies have been conducted on the correlation of hydrogen retention with the bonding,[5–7] conductivity,[8] and field emission[9,10] of diamond films. However, the control of hydrogen content in the diamond films is difficult. The change in electrical properties of MCD films due to heavy ion irradiation will be affected by the hydrogen content in the diamond, which can vary depending on film deposition conditions, and result in some ambiguity in radiation detection. Ultra-nanocrystalline diamond (UNCD) film is a special form of diamond that has recently attracted significant attention from researchers because of its unique granular structure.[11] While the grains of UNCD films have an sp^3 character, the grain-boundaries have a mixture of sp^2, sp^3, hydrocarbon, and amorphous carbon, in which the sp^2 character is predominant.[12,13] This material shows better potential for application as a radiation detector, as the conductivity of the pristine UNCD films can be reliably controlled by carefully adjusting the granular structure of diamond films.

Many reports have discussed the effects of ion beam irradiation on the characteristics of diamond and related materials, such as type IIa diamond,[15] diamond-like carbon films,[16] taC,[17] graphite,[18] and polycrystalline CVD diamond films.[19–21] Pandey *et al.*[22] and Koinkar *et al.*[23] have studied the field emission enhancement by swift heavy ion irradiation in CVD diamonds. The principle of radiation detection in diamond relies on the measurement of electron-hole pairs created within the diamond during the interaction with the incident particles or photons to be detected. The feasibility of using these diamond films as a radiation detector is limited when structural defects are induced by heavy ion irradiation. It is known that the presence of point defects (vacancies) in a semiconductor will lower the mobility of the electrons through the impurity scattering mechanism, and that line defects (dislocations) will act as electron traps that lower the conductivity of the materials by decreasing electron concentration.[14] Moreover, the MCD films contain micron-sized diamond grains with grain boundaries of insignificant thickness, whereas the UNCD films consist of very small diamond grains (~5 nm) with grain boundaries of considerable thickness. The difference in granular structure of these films might influence largely the behavior of the heavy ion irradiation effect for diamond films. Such a phenomenon is still not fully understood.

Here, we report the effect of heavy-ion (2.245 GeV Au) irradiation on altering the granular structure of MCD and

a)Author to whom correspondence should be addressed. Electronic mail: clchang@mail.tku.edu.tw

UNCD films. The modifications to the bonding structure of these films due to heavy ion irradiation were investigated in detail by near edge x-ray absorption fine structure (NEXAFS) using synchrotron radiation and electron energy loss spectroscopy (EELS) in transmission electron microscopy (TEM). Special attention is paid to the comparison of the difference in Au-ion irradiation effects on MCD and UNCD films due to the different microstructures of these materials.

II. EXPERIMENTAL PROCEDURES

The diamond films were deposited via microwave plasma enhanced chemical vapor deposition (MPECVD) using a cylindrical reactor (Innovative Plasma Systems GmbH, CYRANNUS-I). Growth time was 60 min for each film. The film thickness was estimated by cross-sectional scanning electron microscopic (SEM) observation to be around 300 nm for each film. Prior to the deposition of diamond films, the silicon substrates were ultrasonicated in methanol solution, containing nano-diamond powder ($\sim$5 nm) and titanium powder, for 45 min to create nucleation sites. In the growth of MCD films, a gas mixture of CH_4 and H_2 with flow rates of 1 and 99 sccm, respectively, was excited by 1500 W microwave (2.45 GHz). The total pressure in the chamber was maintained at 45 Torr. The substrate temperature was estimated to be around 575 °C during the growth of the MCD films. In contrast, in the growth of UNCD films, a gas mixture of CH_4 and Ar with flow rates of 1 and 99 sccm, respectively, was excited by 1200 W microwave radiation at 2.45 GHz, and the total pressure in the chamber was maintained at 100 Torr. The substrate temperature was estimated to be around 475 °C during the growth of the UNCD films.

The MCD and UNCD diamond films, around 300 nm in thickness, were subjected to 2.245 GeV Au-ion irradiation from the Universal Linear Accelerator (UNILAC) at GSI Helmholtzzentrum für Schwerionenforschung GmbH, Darmstadt, Germany, with fluence of 8.4×10^{13} ions/cm^2. The ion flux of Au for irradiating the diamond films is around 9.38×10^8 ions/cm^2 s over an area about 0.5 cm^2. The 2.245 GeV gold ions have a projected range of 66.4 μm in diamond with longitudinal straggling of 1.93 μm as simulated with SRIM-2008.[24] Therefore, the Au-ions will pass through the diamond films and get buried deep in the substrate for all the samples. There is no doping effect for the diamond films due to the Au-ion irradiation. The Au-ions have an electronic energy loss of 3.34×10^4 eV/nm and a nuclear energy loss of 28.99 eV/nm, which indicates that the ions will lose energy mostly through electronic excitations in the diamond. The lattice damage effects of nuclear energy loss will be minimal. The annealing process was conducted in a 5% H_2/Ar atmosphere at 1000 °C for 1 h.

The films were characterized using SEM (JEOL JSM-6500 F), Raman spectroscopy (Renishaw, excitation wavelength = 514.5 nm), and transmission electron microscopy (Jeol 2100). The detailed microstructure and bonding structure of the samples were examined using EELS (Gatan Enfina) in transmission electron microscopy. The C 1*s* near edge x-ray absorption fine structure measurements were carried out at the Lawrence Berkeley National Laboratory (LBNL), Advanced Light Source (ALS) at beamline 7.0.1. The beamline is equipped with a 99-pole, 5-cm period undulator and spherical grating monochromator. The NEXAFS spectra were obtained in the total electron yield mode by measuring the photocurrent directly from the sample. All the samples measured are conducting reasonably well; thus, no sample charging effect was observed during the experiments. The resolutions were set to 0.1 eV at 290 eV (in the vicinity of the C 1*s* edge). A piece of highly oriented pyrolitic graphite sample was used as the standard samples for energy calibration.

III. RESULTS

A. Effect of Au-ion irradiation on microcrystalline diamond films

Raman spectroscopy is a convenient technique for monitoring the change in bonding structure due to the Au-ion irradiation and annealing processes. Fig. 1 (curve I) indicates that the pristine MCD films contain a sharp D-band resonance peak at 1332 cm^{-1}, the characteristic F_{2g} band for diamond lattices. There are also small broad resonance peaks near 1140 cm^{-1}, 1400 cm^{-1}, and 1580 cm^{-1}, which are associated with the grain boundary trans-polyacetylene (t-PA) phase of nano-sized diamond grains and the disordered carbon.[25–28] However, since the Raman spectroscopy is several times more sensitive to sp^2-bonds than to sp^3-bonds, the presence of sp^2-related Raman resonance peak in the Raman spectroscopy does not mean that the samples contain a large proportion of disordered or graphitic carbons. Au-ion irradiation markedly decreased the intensity of the Raman resonance peaks (curve II), indicating that some proportion of the diamond phase was transformed into a non-diamond phase due to Au-ion irradiation. Annealing the irradiated samples partially restored the Raman resonance peaks (curve III), implying that part of the ion-modified non-diamond phase was re-crystallized into diamond phase. The SEM

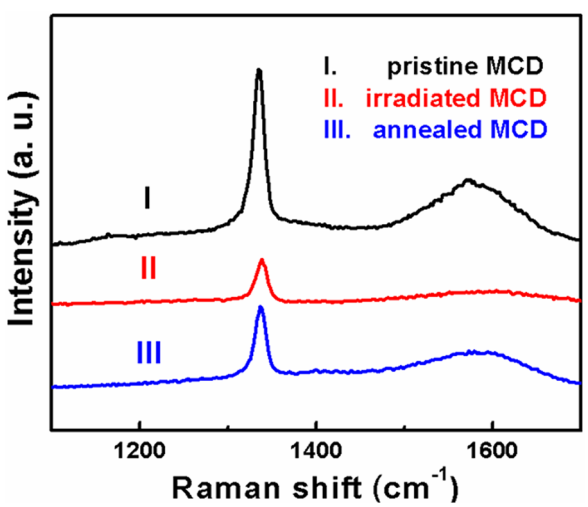

FIG. 1. Raman spectroscopy for the MCD films: (I) pristine, (II) Au-ion irradiated (8.4×10^{13} ions/cm^2), and (III) irradiated/annealed (1000 °C, 1 h).

investigation that is not shown here indicates that the Au-ion irradiation markedly reduced the size of the grains from 900 nm for pristine MCD films to around 300 nm and converted the faceted surface morphology for diamond grains of the pristine MCD films to roundish in geometry. Annealing of the Au-ion irradiated films resumed the faceted geometry, but the diamond grains are still around 300 nm.

To understand how the Au-ion irradiation/annealing processes alter the characteristics of the diamond films, more detailed bonding structures were analyzed by NEXAFS and EELS in TEM. In Fig. 2(a), the NEXAFS spectra are presented. From bottom to top: the pristine MCD film (curve I), the Au-ion irradiated film (curve II), and the irradiated/annealed film (curve III). Starting with the pristine film, the spectra can be divided into two regimes, a prominent peak at ~285.3 eV and a relatively broad feature between ~290 and 303 eV. The former is assigned to the unoccupied π^* bond, which is characteristic of the sp^2 C=C bond. The latter is due to σ^* bond, which is characteristic of the sp^3 tetrahedral C–C bond. The peak at ~289.5 eV corresponds to the diamond core exciton, which is the result of the bound electron-hole pair. The dip at ~302.5 eV is attributed to the second absolute band gap. Both are characteristics of NEXAFS spectrum corresponding to the diamond of Fd3m structure.

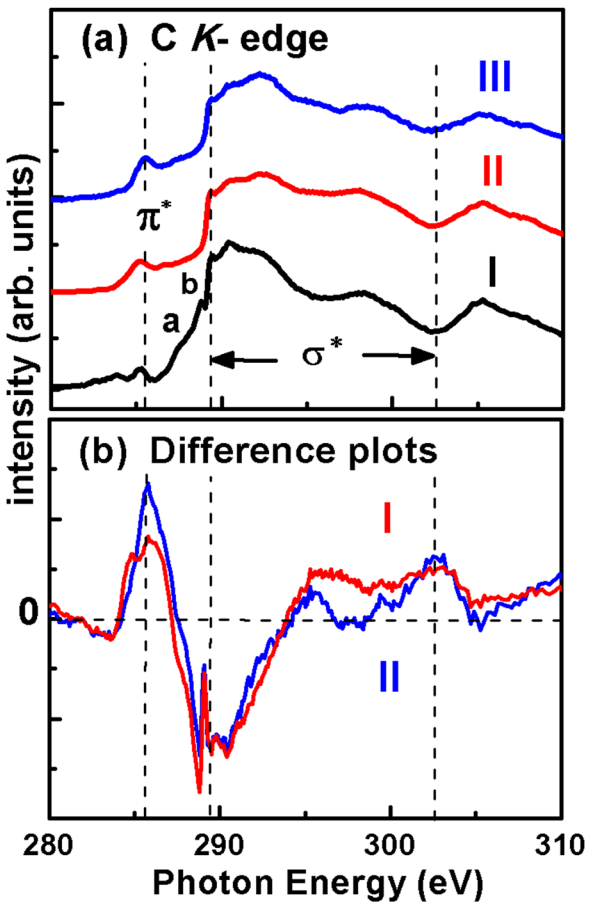

FIG. 2. (a) NEXAFS of MCD films, (I) pristine, (II) Au-ion irradiated (8.4×10^{13} ions/cm^2), and (III) irradiated/annealed (1000 °C, 1 h); (b) spectral difference constructed by (I) subtracting NEXAFS of pristine film from that of Au-ion irradiated film and (II) subtracting NEXAFS of pristine film from that of irradiated/annealed film.

The exciton peak and the dip are often used to evaluate the quality of diamond.[29] Moreover, two weak bumps *a* (at ~287.5 eV) and *b* (at ~288.8 eV) are observed between the π^* and σ^* bonds. Feature *a* is attributed to the C–H bond, feature *b* is due to the C=O bond. The C–H bond originates from the absorption of hydrocarbon to the dangling bonds at grain boundaries during the film deposition process,[30] while the C=O bond is likely due to residual water vapor during the growth.[31] There are different reports regarding the origin of the pre-edge feature appearing below the π^* peak at about 282.5 eV. A couple of groups[32,33] have ascribed it to the C 1*s* exciton located at the surface of diamond grains, i.e., the grain boundaries, while other reports have speculated that it originates from disordered carbon.[34,35]

In the Au-ion irradiated film the intensity of the sp^2 feature (π^* at ~285.3 eV) is slightly increased, while a significant broadening of the peak (FWHM increases by 73% compared to the pristine film) is observed. The broadening of the sp^2 feature in irradiated film indicates the decrease in the ordering of sp^2-bonds, i.e., the formation of amorphous carbon.[33,36] In the meantime the relative intensity of the characteristic sp^3 feature, the diamond exciton peak (~289.5 eV), and the depth of the second band gap dip (~302.5 eV) are reduced indicating a noticeable structural modification away from Fd3m structure, i.e., the creation of point or line structural defects. Also observed is the disappearance of the pre-edge feature at about 282.5 eV, and bumps *a* and *b*, which indicates that most of the constituents formed at the grain boundaries are removed upon high energy Au-ion irradiation. The spectrum of the irradiated/annealed sample (III) is similar to the spectrum II, and the main difference observed is the feature ~285.3 eV (π^* peak) is increased for the case of the irradiated/annealed sample. Furthermore, the FWHM for the irradiated/annealed sample is reduced to within 18% of that of the pristine film, which indicates an increase in the ordering of sp^2-bonded structure (or recrystallization of amorphous carbon into graphitic phase) with annealing.

The effect of Au-ion irradiation and the subsequent annealing on the NEXAFS spectra can be emphasized by subtracting the spectrum of the pristine film from the respective spectra. The difference plots are shown in Fig. 2(b). The red curve (I) is the spectral difference of the irradiated film to the pristine film and the blue curve (II) is that of the irradiated/annealed film to the pristine film. The peaks in the red curve are the features mainly originating from the Au-ion irradiation, and the dips are the features that have been reduced by the ion irradiation. The prominent feature near 285.3 eV (π^* peak) indicates the increase of the amount of graphite contribution. The prominent shoulder at 284.8 eV indicates the development of a considerable amount of amorphous carbon (a-C).[37] The sharp dip at 288.8 eV indicates a decrease in amount of the C=O bonding in the surface.[38] The other dip at 289.5 eV (designated by dotted line) indicates the weakening of the exciton peak, due to the point defects created by the Au-ion irradiation.[39] The negative intensity above this dip indicates the reduced σ^* (sp^3) contribution. The positive intensity between 295 and 302 eV is due to the broad a-C contribution.[40] The peak at 302.5 eV is

evidence of the significantly reduced magnitude of the absolute second band gap dip, which indicates that the Au-ion irradiation generates defective crystalline structure in the diamond grains.[41] The effect of the annealing on the Au-ion irradiated MCD film is revealed by comparing the red curve (I) and the blue curve (II) in Fig. 2(b). Two major differences are observed. First, the intensity between 295 and 302 eV is less for curve II. Second, the intensity of the graphite peak near 285.5 eV in curve (II) is enhanced while the shoulder to the lower energy side cannot be distinguished. Evidently, the annealing process not only decreased the proportion of structural defects (or the amount of a-C) but also increased the graphitic structure in the film.

While the NEXAFS provides valuable information on the evolution of bonding structure for the MCD films due to Au-ion irradiation and annealing processes, how such processes affect the granular structure of the films locally is still not fully understood. To examine the local modification of the granular structure, the samples were investigated using EELS in TEM. Fig. 3(a) shows the typical granular structure of the pristine MCD films, wherein only the grains oriented near some zone-axes strongly diffract electrons and show high contrast. The adjacent grains are oriented away from any zone-axis, showing low contrast. The diffraction spots in the selected area electron diffraction (SAED) patterns (inset in Fig. 3(a)) are arranged nearly around a ring geometry, indicating that the MCD grains are randomly oriented.

Au-ion irradiation markedly alters the microstructure of the MCD films. Fig. 3(b) shows that, for the as-irradiated MCD films, in addition to the large diamond grains, which survive the ion irradiation and still preserve good crystallinity (region B_1), there are regions that consist of small clusters (region B_2). SAED shown as inset in Fig. 3(b) indicates that there are weak diffraction rings, corresponding to randomly oriented small diamond grains, as well as strong discrete diffraction spots corresponding to large diamond grains. The weak diffraction ring indicates that crystallinity of the small diamond grains has been degraded due to the Au-ion irradiation process. Fig. 3(c) shows that the irradiated/annealed MCD films also contain bimodal granular structure, viz., they consist of a mixture of large-grain and small-grain regions, which are designated as regions C_1 and C_2, respectively. The SAED (inset, Fig. 3(c)) contains diffraction rings, instead of diffraction spots, implying that the small diamond grain regions are larger in proportion than the large diamond grain regions. The intensity of the diffraction rings increases compared to those for the as-irradiated films, indicating that the nano-sized clusters have been recrystallized due to the annealing process. There is a diffused ring in the center of SAED, indicating the presence of some amorphous carbon (or graphitic phase) for the film. Moreover, clear extra diffraction rings are present beside the diamond (111), (220), and (311) diffraction rings, indicating that large proportion of secondary phase was created by the annealing process. Apparently, the secondary phase, which is presumably the *i-carbon*, the bcc structured carbon with $a_0 = 0.432$ nm,[42] was recrystallized from the amorphous-carbon phase by the Au-ion irradiation.

The selected area EELS spectra corresponding to the labeled regions in Fig. 3 are shown in Fig. 4. The curves I, II, and III in Fig. 4(a) are the carbon core-loss spectra corresponding to regions A of pristine, B_1 of Au-ion irradiated, and C_1 of irradiated/annealed films, respectively. These spectra show a prominent σ^*-band near 292 eV with a large dip near 303 eV. The π^*-band near 285.5 eV is not observable. These features are essentially the same as the NEXAFS spectra shown in Fig. 2(a), except that the σ^*-band in EELS is not as sharp as those in NEXAFS. The roundness of the σ^*-band in EELS is presumably due to the interaction of

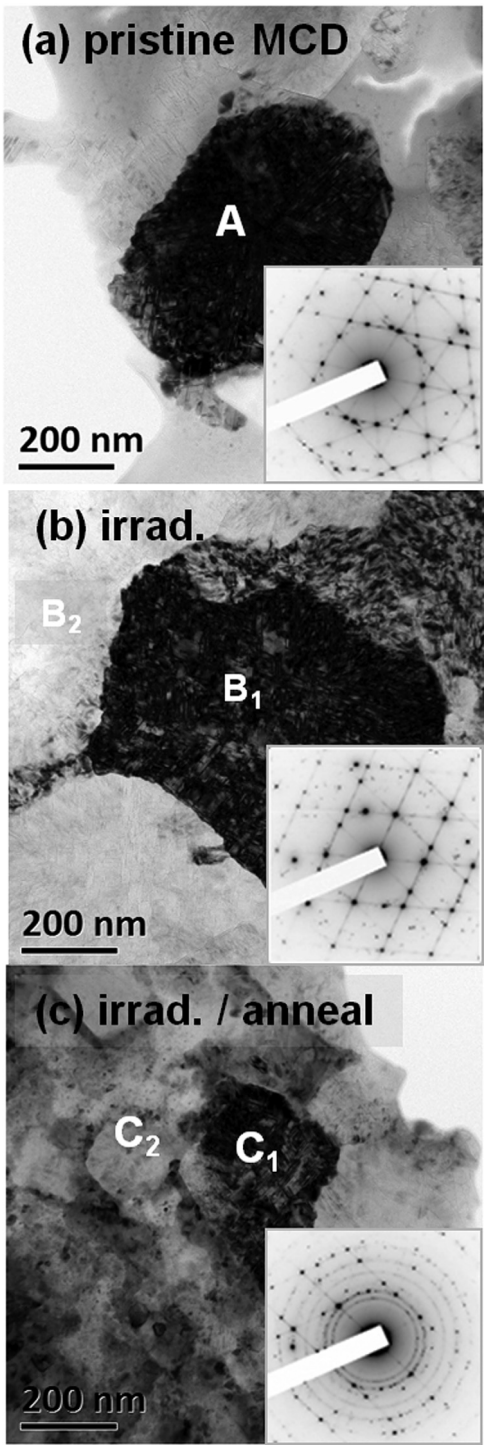

FIG. 3. TEM bright field micrographs for (a) pristine, (b) 8.4×10^{13} ions/cm^2 Au-ion irradiated, and (c) 1000 °C(1 h) irradiated/annealed MCD samples. The insets show the corresponding SAED.

electrons with the surface bonding in diamond films. These EELS spectra clearly indicate that these regions are predominated with diamond.[42,43] Curve IV in Fig. 4(a) is the core-loss EELS corresponding to the small grain region (B_2) of the Au-ion irradiated samples. In addition to the σ^*-band and the dip, a small π^*-band near 285.5 eV is readily observed indicating the existence of sp^2 C=C bonded amorphous carbon along with diamond in this region. Curve V in Fig. 4(a) is the core-loss EELS corresponding to the small grain region (C_2) of the irradiated/annealed samples. The σ^*-band and the dip, both characteristics of sp^3-tetrahedral C–C bond, were completely demolished. The π^*-band near 285.5 eV becomes markedly lager indicating that the materials in this region have been transformed into other non-diamond phases.

The plasmon-loss EELS spectra near 15-40 eV shown in Fig. 4(b) provide more insight of the phase constituents in these samples. The broaden peaks can be deconvoluted using Gaussian function in the vicinity of s_1 (22 eV), s_2 (23 eV), s_3 (27 eV), and s_4 (33 eV), as these peaks are the plasmon-loss peaks corresponding to the possible phases contained in diamond materials. Notably, the signature of the plasmon-loss EELS spectra corresponding to diamond consists of a broad peak centered at 33 eV (s_4-band) with a prominent shoulder at 23 eV (s_2-band), which are due to the bulk plasmon and surface plasmon, respetively.[42] The peak ratio of s_2 to s_4 peaks is about $1:\sqrt{2}$. On the other hand, the main features of graphite consist of a peak at 7 eV (not observed in our spectra) due to π electrons alone, and a peak at 27 eV (s_3-band) due to all the valence electrons.[42] The plasmon-loss peak at 22 eV (s_1-band) is less well-founded. Prawer *et al.*[43] assigned this peak as the plasmon of an allotropy phase of diamond with a body-centered-cubic structure, also known as *i-carbons*.

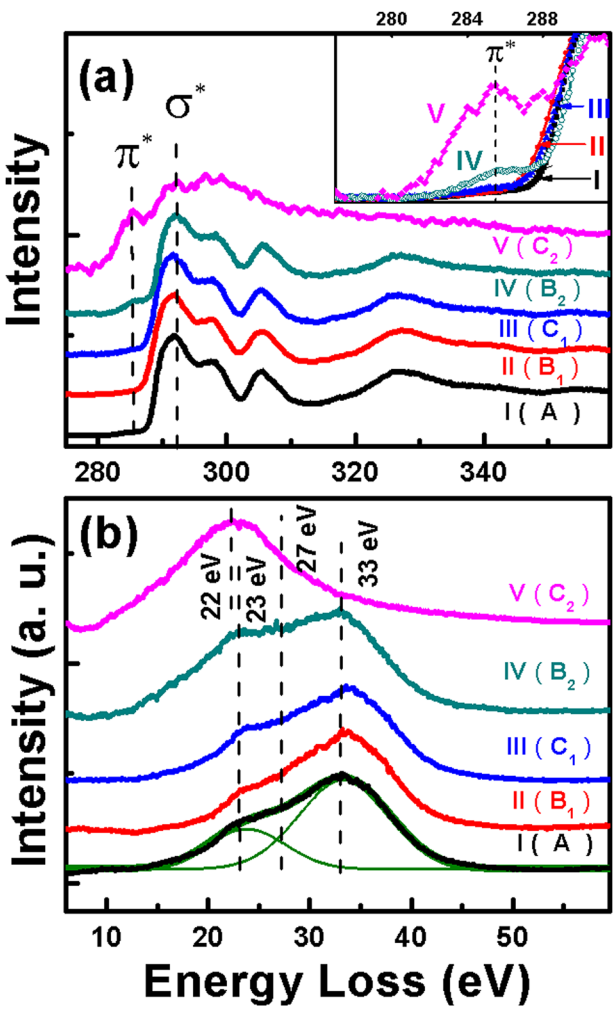

FIG. 4. Selected area EELS spectroscopy of MCD films: (a) core-loss EELS spectra, the enlarged region near π^*-band is plotted in the inset. (b) The plasmon-EELS spectra; (I) the pristine, (II) Au-ion irradiated (region B_1 in Fig. 3(b)), (III) Au-ion irradiated/annealed (region C_1 in Fig. 3(c)), (IV) Au-ion irradiated (region B_2 in Fig. 3(b)), and (V) Au-ion irradiated/annealed (region C_2 in Fig. 3(c)).

Curve I of Fig. 4(b) clearly indicates that the pristine film (region A) is diamond of Fd3m structure, as it contains s_2- and s_4-bands with intensity ratio of $\sim 1:\sqrt{2}$. The spectral shapes of curves II and III are similar to curve I, which indicates that region B_1 of Au-ion irradiated sample and region C_1 of irradiated/annealed sample are predominated with diamond.

Curve IV in Fig. 4(b) is also predominated with s_4-band (33 eV) but with a significantly larger shoulder. Since the intensity ratio of surface plasmon of diamond (the s_2-band at 23 eV) is supposed to be fixed relative to the bulk plasmon of diamond (the s_4-band at 33 eV), the increase in the intensity of the shoulder in the vicinity of 22–23 eV is attributed to the presence of s_1-band (22 eV). The emergence of s_1-band indicates that some of the materials in region B_2 in Au-ion irradiated films were transformed into non-diamond phase. In contrast, the broad peak in curve V (Fig. 4(b)) can be assigned to s_1-band at 22 eV, since the s_2-band (23 eV) should be completely non-observable if the samples contain no diamond (i.e., no s_4-band at 33 eV). The dramatic alteration of the spectral shape observed in curve V can accordingly be attributed to the absence of diamond phase and the formation of a non-diamond phase, *i-carbon*,[43] in the irradiated/annealed sample.

B. Effect of Au-ion irradiation on the UNCD films

The above observations and previous studies indicate that the granular structure of MCD films can be significantly modified if the irradiating Au beams possess sufficiently high energy and large fluence.[44] The Au-ion irradiation induced the breakdown of some large diamond grains into nano-sized diamond clusters when the fluence of Au ions exceeded a certain limit. On the other hand, the UNCD films consist of ultra-small diamond grains ($\sim$5 nm) with abundant grain boundaries. These grain boundaries, which are of considerable thickness and contain trans-polyacetylene (or amorphous carbon) materials, are expected to be more susceptible to the ion irradiation damage.

The general effects of Au-ion irradiation on the characteristics of the UNCD films, studied by Raman spectroscopy, are shown in Fig. 5. This figure indicates that the bonding structure of these films was markedly modified due to Au-ion irradiation and annealing processes. The Raman spectrum of the pristine UNCD films (curve I) contains ν_1-band

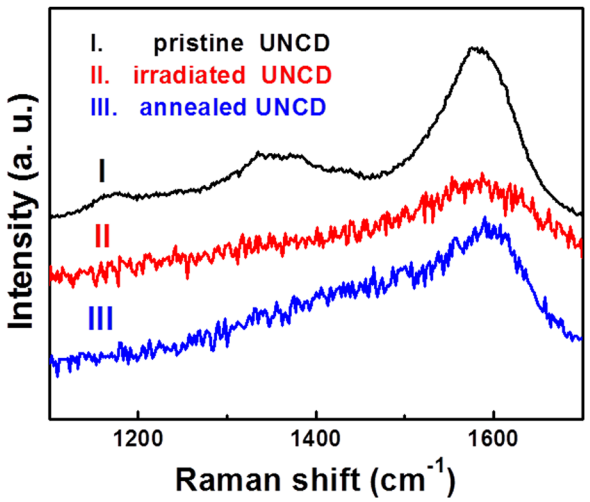

FIG. 5. Raman spectroscopy for the UNCD films: (I) pristine, (II) Au-ion irradiated (8.4×10^{13} ions/cm^2), and (III) irradiated/annealed (1000 °C, 1 h).

($1140\,cm^{-1}$) and ν_2-band ($1480\,cm^{-1}$) resonance peaks, which correspond to trans-polyacetylene at the grain boundaries,[25,26] and D*-band ($1350\,cm^{-1}$) and G-band ($1580\,cm^{-1}$) resonance peaks, which correspond to disordered carbon.[27,28] These Raman spectra are characteristic of UNCD films with ultra-small grains. The D-band ($1332\,cm^{-1}$) resonance peaks, which correspond to the F_{2g} resonance mode of the 3 C diamond lattice with Fd3m symmetry, are only barely visible. The Raman spectra are markedly altered due to the Au-ion irradiation. Curve II shows that all the resonance peaks corresponding to UNCD materials are diminished, replaced by a noisy signal with a broadened peak near $G^* = 1580\,cm^{-1}$, characteristic of the nano-sized graphite. This result implies that a large proportion of sp^2-bonds were induced. Again, because visible Raman spectroscopy is more sensitive to sp^2-bonds than to sp^3-bonds, an sp^2 signal overwhelmingly larger than the sp^3 signal does not indicate that all the sp^3-bonded materials have been converted into sp^2-bonded materials. The Raman spectra were only moderately altered by the post-irradiation annealing process, i.e., the Raman signal was still noisy, and contained only the G-band resonance peak at $1580\,cm^{-1}$, which was slightly narrower (curve III). The Au-ion irradiation barely altered the SEM morphology of the UNCD films (not shown). Only deep grooving was observed, implying that the grain boundary phase, the trans-polyacetylene, in UNCD films was dissociated due to Au-ion irradiation process. There are no significant modifications observed in the SEM morphology after annealing of the Au-ion irradiated films at 1000 °C (1 h).

Again, NEXAFS and EELS investigations are needed for the purpose of understanding the genuine factor that influences the characteristics of the UNCD films due to Au-ion irradiation and the annealing processes. Fig. 6(a) plots C *K*-edge NEXAFS spectra of UNCD films, from bottom to top, the pristine film (curve I), the Au-ion irradiated film (curve II), and the irradiated/annealed film (curve III). The spectrum of the pristine film is much the same as that of the MCD film except for a much weaker exciton peak, which is due to the smaller grain size.[35,45] The pre-edge peak, the

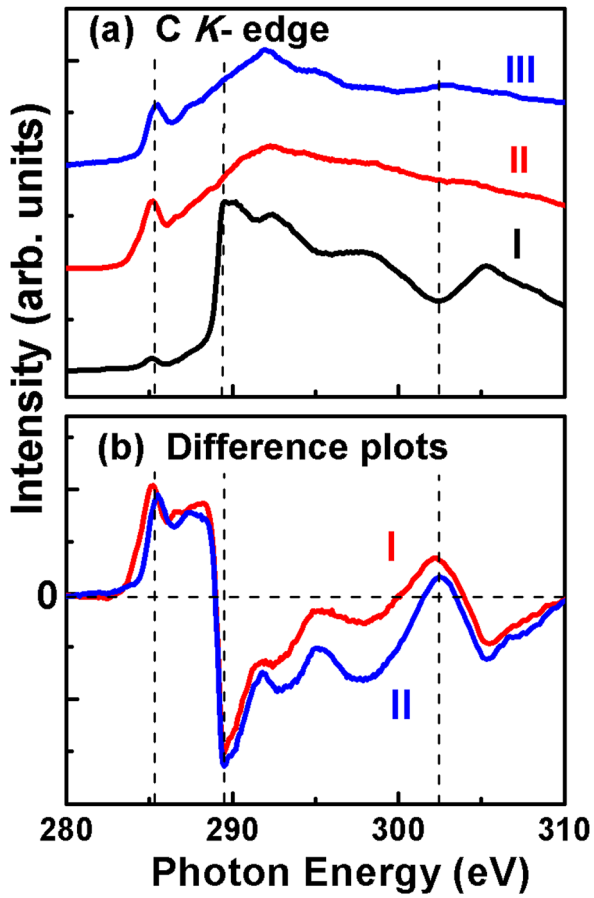

FIG. 6. (a) NEXAFS of the UNCD films, (I) pristine, (II) Au-ion irradiated (8.4×10^{13} ions/cm^2), and (III) irradiated/annealed (1000 °C, 1 h); (b) spectral difference constructed by (I) subtracting NEXAFS of pristine film from that of Au-ion irradiated film and (II) subtracting NEXAFS of pristine film from that of irradiated/annealed film.

C=O and C–H peaks are not present in UNCD film. This may be due to a different growing process. The spectral shape of the irradiated film shows marked differences. The sp^2 peaks are enhanced; the exciton peaks and the second band gap dips disappeared. Also observed is the apparent loss of absorption structures in the range of 290 and 310 eV after Au-ion irradiation, which is associated with the loss of long-range order.[33] The spectral shape of the irradiated/annealed film is similar to that for the irradiated film.

The difference plots were created by the same process to those for the MCD films, and are shown in Fig. 6(b). We first focus our attention on the red curve (I) to study the effect of Au-ion irradiation. The sp^2 feature at 285.3 eV is largely enhanced, broadened, and slightly shifted to the lower energy side, which is due to the increased amount of disordered sp^2-bonded carbon. A small peak at 286.8 eV is also related to amorphous carbon. The broad peak at 288.3 eV was reported by Jeong *et al.*, based on the study of oxygenated diamond surface, and ascribed to O=C bonding.[38] Other reports have assigned this feature to be originated from the defect induced surface states, based on the studies on ion beam damaged diamond surface[36] and the unoccupied states at diamond surface.[30] We have performed O *K*-edge x-ray absorption spectra (not shown), for contamination

monitoring purposes, which display no significant changes in the Au-ion irradiated sample or irradiated/annealed sample relative to the pristine sample. Moreover, the corresponding C=O peak at ~535 eV[45,46] is not present in our O *K*-edge data. We therefore assign this feature to the defect-induced unoccupied surface states. The big dip at 289.5 eV shows that the exciton peak is diminished upon irradiation. The loss of the exciton peak may be caused by the decreased core hole life time originating from the confinement of the electron and core hole in the extremely small diamond particles (<5 nm), which emerged from the collapsed UNCD grains.[47] The peak at 302.5 eV indicates the loss of the absolute second band gap dip indicating the loss of diamond long range order.[48] The post-annealing effect can be studied by comparing the blue curve (II) with the red curve (I). For curve II (the annealed UNCD films) the sp^2 peak is considerably less intense with a noticeable shift to the higher energy side, which indicates that the amount of disordered sp^2-bonded carbon is reduced after the annealing.[10] The other obvious change is that the intensity at 287.3 eV is obviously higher than that at 288.3 eV in curve (II), indicating that the annealing has reduced the surface states and generated more C–H bonding at the surface.

On the other hand, Fig. 7 shows the evolution of the microstructure of UNCD films resulted from the Au-ion irradiation and annealing processes. Figs. 7(a) and 7(b) show, respectively, the bright field TEM micrographs for the pristine and as-irradiated UNCD films, indicating that the microstructures of the two films are quite similar. But more detailed examinations show that the diamond aggregates contained in the Au-ion irradiated films are larger and more obvious. Moreover, the aggregates within Au-ion irradiated films cannot be separated due to electron irradiation during TEM examination, implying that these aggregates are hard agglomerates. In contrast, the aggregates in the pristine UNCD films were separated easily due to electron irradiation during TEM examination, indicating that these aggregates are soft agglomerates. On the other hand, Figs. 7(c) and 7(d) show two typical regions of the Au-ion irradiated/annealed UNCD films. These microstructures are very similar with one another. Annealing the Au-ion irradiated films seems not to markedly alter the population of diamond aggregates. However, more detailed analyses reveal a marked difference in the granular structure of these regions. SAED in the inset of Fig. 7(d) contains the diffraction rings larger than the typical (111) diamond ring (cf. inset, Fig. 7(c)). Such a diffraction ring corresponds to *i-carbon*, the bcc structured carbon.[42] Presumably, *i-carbon* particulates were re-crystallized from the amorphous carbon during annealing process. The nano-sized graphite is always present along with the formation of *i-carbon* that is inferred by the presence of a strong central diffuse ring in the SAED of Fig. 7(d).

Fig. 8 plots the selected area EELS spectra corresponding to the TEM micrographs in Fig. 7. The curves I and II in Fig. 8(a) are the carbon core-loss spectra for the pristine and Au-ion irradiated UNCD films, corresponding to Figs. 7(a) and 7(b), respectively. These curves exhibit typical EELS spectra of diamond with Fd3m structure, as they contain a σ^*-band near 292 eV and a large dip near 310 eV. The

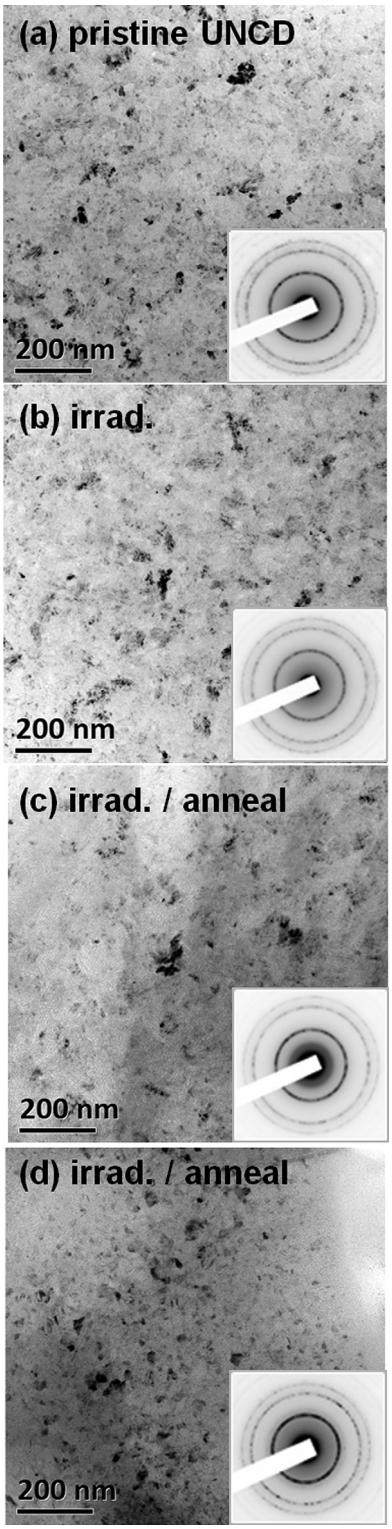

FIG. 7. TEM bright field micrographs of the UNCD films with the insets showing the SAED patterns. The samples were (a) pristine, (b) Au-ion irradiated (8.4×10^{13} ions/cm^2) and (c, d) irradiated/annealed (1000 °C, 1 h), where (c) is regularly phase transformed region and (d) is the irregularly phase transformed region.

σ^*-band for the UNCD films is not as sharp compared to the spectra for MCD (cf. Fig. 4) indicating that there is a larger proportion of distorted sp^3-bonds located at the surface of the ultra-small diamond grains. Moreover, there are prominent π^*-bonds in both of the core-loss EELS spectra

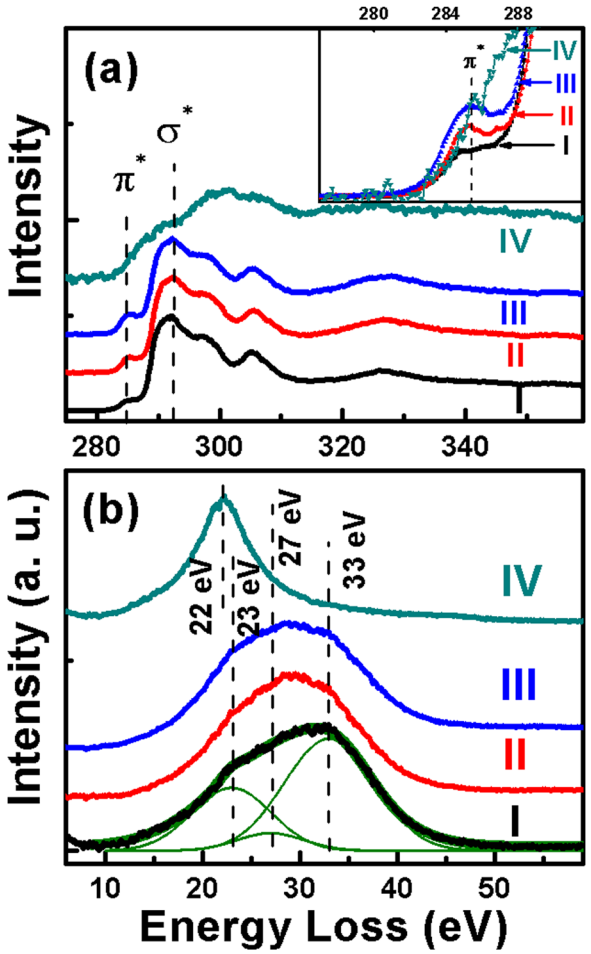

FIG. 8. Selected area EELS spectroscopy of UNCD films: (a) core-loss EELS spectra and (b) the plasmon EELS spectra, where the enlarged region near π*-band is plotted in the inset of "a"; (I) the pristine, (II) Au-ion irradiated, (III) Au-ion irradiated/annealed spectrum corresponds to the regularly phase transformed region in Fig. 7(c), and (IV) Au-ion irradiated/annealed spectrum corresponds to the irregularly phase transformed region in Fig. 7(d).

indicating the presence of trans-poly-acetylene phase in the grain boundary regions. The peak intensity of π*-bonds is larger for the Au-ion irradiated samples. Such a phenomenon is more clearly illustrated in the enlarged EELS near the π*-band (~285 eV), plotted in the inset of Fig. 8(a).

Curves III and IV in Fig. 8(a) show the core-loss EELS spectra corresponding to the regularly phase-transformed and the irregularly phase-transformed regions of the irradiated/annealed UNCD films, which correspond to Figs. 7(c) and 7(d), respectively. Curve III is very similar to the core-loss EELS spectrum of diamond (cf. curves I or II), indicating that the regularly phase-transformed region also is dominated with diamond. The π*-band in this curve is larger in intensity than that of curves I and II implying that this region contains larger proportion of graphitic (or amorphous carbon). Curve IV is markedly different from all the other curves and it is similar to the core-loss EELS spectrum corresponding to C_2-region of the irradiated/annealed MCD sample (cf. curve V, Fig. 4(a)), which indicates that the phase contained in this region is mainly *i-carbon*.

Fig. 8(b) shows the plasmon loss EELS spectra of the same regions. It is observed that curve I is dominated with the bulk plasmon loss (s_4, 33 eV)) and the surface plasmon loss (s_2, 23 eV) indicating again that pristine UNCD films are mainly diamond. Also observed is that this curve contains an additional small peak near 27 eV (s_3-band) indicating that the pristine UNCD film contains some sp^2-bonded phase (graphite or amorphous carbon) besides diamond, which is in accord with the TEM observations. Curve II shows the plasmon-loss EELS of Au-ion irradiated UNCD films, which indicates that s_2- and s_4-bands still dominate with increased spectral weight of s_3-band compared to curve I. This result indicates that Au-ion irradiation causes increased content in graphite (or a-C) phase. Curves III and IV in Fig. 8(b) show the plasmon-loss EELS spectra corresponding to the regularly phase-transformed (cf. Fig. 7(c)) and the irregularly phase-transformed (cf. Fig. 7(d)) regions of the irradiated/annealed UNCD films, respectively. Curve III is also dominated with the bulk plasmon loss (s_4-band) and the surface plasmon loss (s_2-band) of diamond, but with larger s_3-band (~27 eV) than that of curves I and II indicating that this region consists of a larger proportion of sp^2-bonded phase (graphite or amorphous carbon) besides diamond. Notably, the plasmon-loss peaks corresponding to amorphous carbon are very similar to those for graphite, and they are not clearly identifiable by plasmon-loss EELS spectra.[42] TEM investigation is needed to differentiate these phases. In contrast, curve IV shows a plasma-loss EELS spectrum corresponding to the irregularly phase-transformed region that is totally different from that of the regularly phase-transformed region (cf. curve III, Fig. 8(b)). There is only a large s_1-band (~22 eV) observed. No characteristic bulk plasmon-loss peaks of diamond were observable. It should be reminded that the surface plasmon of diamond, s_2-band (~23 eV) is associated with the bulk plasmon of diamond, s_4-band (~33 eV). The disappearing of the diamond phase infers that there is no s_2-band (~23 eV) in this curve. Hence, the plasmon-loss peak present in curve IV can be assigned to the carbon phase other than diamond, in accord with the TEM observations. Therefore, we ascribe the presence of s_1-band (~22 eV) to the formation of *i-carbon*.[43]

The above-mentioned results imply that the Au-ion irradiation process altered the granular structure of the UNCD films in a non-uniform manner. In some regions, the UNCD diamond lattices are only moderately defected. The annealing process healed the defects and induced the growth of grains. In other regions, the UNCD diamond grains are seriously damaged such that the annealing process has triggered the phase transformation toward a more stable phase, the sp^2-bonded graphite. The *i-carbon* is an intermediated phase, which was induced in accompaniment with the formation of nano-sized graphite. Such observations account for the modification observed in the NEXAFS spectra caused by the Au-ion irradiation/annealing processes. The nano-sized graphite/*i-carbon* regions are large in proportion such that the characteristics of the NEXAFS spectra, with sampling area of hundreds of square microns, were altered markedly (cf. spectra II and III, Fig. 6(a)) and were completely different from those of diamond materials (cf. spectrum I, Fig. 6(a)).

IV. DISCUSSION

Amidst carbon materials, it would be expected that diamond would be most radiation-hard. However, when the fluence of Au-ions exceeded a certain limit, some of the large grains were broken into smaller gains and some of them were even disintegrated into nano-sized clusters.[44] These regions contain nano-sized diamonds embedded in a matrix of amorphous carbon with a small proportion of *i-carbon*. Annealing the Au-ion irradiated films healed partially the planar defects in the diamond grains and converted the amorphous carbon into crystalline nano-particulates, including nano-diamond, *i-carbon*, and nano-sized graphites. The proportion of *i-carbon* in the annealed films increased markedly, compared with the as Au-ion irradiated films. The Au-ion irradiation and annealing processes modify the granular structure of the UNCD films in a different way from that on the microstructure of the MCD films. Au-ion irradiation altered the granular structure of UNCD films nonuniformly. While in some of the regions the granular structure was hardly altered, in other regions, a large proportion of a-C phase was induced. This a-C was converted into nano-sized graphite and *i-carbon* clusters during the annealing process.

Generally, for a polycrystalline diamond material, carbon atoms in the grain boundaries are not bonded as strongly as those in the bulk materials. Therefore, the grain boundary regions are more susceptible than the bulk regions to damage by incident high energy heavy ions. The difference in the ion irradiation effect on the modification of the granular structure of the MCD and UNCD films is probably due to the different microstructures of the two types of films. The grain boundaries of the MCD films are sharp and contain no amorphous carbon. In this case, Au ions can only impose irradiation damage on the diamond lattices, which requires large dissociation energy. The kinetic energy of the Au ions is only sufficient to disintegrate the diamond grains into smaller diamond grains (or to nano-sized clusters) with the amorphous carbon as a byproduct. The thermal spike is not sufficient for crystallization of the a-C phase into graphite. High temperature annealing process is required to repair the atomic defects in the diamond grains and convert the amorphous carbon located between the diamond grains into nano-sized graphite (or *i-carbon*).

In contrast, the UNCD films contain nano-sized diamond grains with abundant grain boundaries of considerable thickness. The nano-sized grains are not further disintegrated by the irradiation of the kinetic Au ions. Most of the kinetic energy of the Au ions acted on dissociating the hydrocarbons in the grain boundaries and produced large transient thermal spikes that induced *in situ* re-crystallization of the grain boundary phases into nano-sized graphite. The dissociation of hydrocarbons produced highly active carbon, which was able to attach to the nano-sized diamond grains, inducing the coalescence of nano-sized diamond grains into large aggregates. In the meantime, homogeneous nucleation of graphite clusters occurred. The Ostwald-ripening and homogeneous nucleation processes are readily triggered by the Au-ion irradiation process in UNCD films but not in MCD films. The annealing process converts the heavily damaged nano-diamond into *i-carbon* particulates.

The above observations indicate that irradiation with heavy ions of sufficiently high energy and large fluence (i.e., $\geq 8.4 \times 10^{13}$ ions/cm^2) will result in apparent change in the granular structure for the diamond films, regardless the grain size (MCD or UNCD). This phenomenon indicates the regime where the diamond films are not suitable for radiation detector application. However, it may be appropriate to apply MCD and UNCD films for radiation detection if the kinetic energy or fluence of the incident ions does not exceed the limit.[44]

V. CONCLUSION

The effect of 2.245 GeV Au-ion irradiation and annealing processes on altering the microstructure of MCD and UNCD films was investigated using NEXAFS and EELS in TEM. These examinations revealed that for MCD films, Au-ion irradiation disintegrated some of the diamond grains, resulting in nano-sized diamond particulates embedded in amorphous matrix. Annealing process recrystallized the diamond grains and converted the amorphous carbon into nano-sized crystalline graphite. In contrast, for UNCD films, the Au-ion irradiation did not significantly alter the crystallinity of the grains of the UNCD films, but the grain boundary phase was transformed into nano-sized graphite. The phase transformation induced by the Au-ion irradiation/annealing processes is not uniform. In some regions, the irradiation/annealing processes recrystallized the residual a-C phase into nano-sized graphites, whereas in other regions, it induced the formation of *i-carbon*. The difference in microstructural evolution behavior for MCD and UNCD films is intimately correlated to their different granular structure.

ACKNOWLEDGMENTS

We acknowledge Dr. Balakrishnan Sundaravel, Dr. Sankarakumar Amirthapandian, Dr. Christina Trautmann, and the Materials Research Group of GSI, Darmstadt for their support during GeV irradiation at the XO beamline of the UNILAC. Financial support granted by the National Science Council of Republic of China through Project Nos. NSC 100-2112 -M-032-004 and NSC 101-2112 -M-032-002 is gratefully acknowledged by the authors.

[1]S. F. Kozlov, E. A. Konorova, Y. A. Kuznetsov, Y. A. Salikov, V. I. Redko, V. R. Grinberg, and M. L. Meilman, IEEE Trans. Nucl. Sci. **24**, 235 (1977).
[2]G. Faggio, M. Marinelli, G. Messina, E. Milani, A. Paoletti, S. Santangelo, and G. V. Rinati, Microsyst. Technol. **6**, 23 (1999).
[3]P. Bergonzo, A. Brambilla, D. Tromson, C. Mer, B. Guizard, F. Foulon, and V. Amosov, Diamond Relat. Mater. **10**, 631 (2001).
[4]P. Bergonzo, D. Tromson, and C. Mer, Semicond. Sci. Technol. **18**, S105–S112 (2003).
[5]Sh. Michaelson, O. Ternyak, R. Akhvlediani, A. Hoffman, A. Lafosse, R. Azria, O. A. Williams, and D. M. Gruen, J. Appl. Phys. **102**, 113516 (2007).
[6]C. J. Tang, M. A. Neto, M. J. Soares, A. J. S. Fernandes, A. J. Neves, and J. Grácio, Thin Solid Films **515**, 3539 (2007).
[7]P. Reichart, G. Datzmann, A. Hauptner, R. Hertenberger, C. Wild, and G. Dollinger, Science **306**, 1537 (2004).
[8]P. W. May, W. J. Ludlow, M. Hannaway, P. J. Heard, J. A. Smith, and K. N. Rosser, Chem. Phys. Lett. **446**, 103 (2007).

[9]S. G. Wang, Q. Zhang, S. F. Yoon, J. Ahn, Q. Wang, Q. Zhou, and D. J. Yang, Phys. Status Solidi A **193**, 546 (2002).
[10]K. H. Wu, E. G. Wang, Z. X. Cao, Z. L. Wang, and X. Jiang, J. Appl. Phys. **88**, 2967 (2000).
[11]T. D. Corrigan, D. M. Gruen, A. R. Krauss, P. Zapol, and R. P. H. Chang, Diamond Relat. Mater. **11**, 43 (2002).
[12]J. Birrell, J. A. Carlisle, O. Auciello, D. M. Gruen, and J. M. Gibson, Appl. Phys. Lett. **81**, 2235 (2002).
[13]B. Dischler, C. Wild, W. M. Sebert, and P. Koidl, Physica B **185**, 217 (1993).
[14]S. M. Sze, *Physics of Semiconductor Devices* (John Wiley and Sons, 1969).
[15]S. Prawer and R. Kalish, Phys. Rev. B **51**, 15711 (1995).
[16]J. Krauser, J.-H. Zollondz, A. Weidinger, and C. Trautmann, J. Appl. Phys. **94**, 1959 (2003).
[17]N. Koenigsfeld, H. Hofsäss, D. Schwen, A. Weidinger, C. Trautmann, and R. Kalish, Diamond Relat. Mater. **12**, 469 (2003).
[18]S. Prawer, A. Hoffman, and R. Kalish, Appl. Phys. Lett. **57**, 2187 (1990).
[19]W. Zhu, G. P. Kochanski, S. Jin, L. Seibles, D. C. Jacobson, M. McCormack, and A. E. White, Appl. Phys. Lett. **67**, 1157 (1995).
[20]N. Dilawar, R. Kapil, V. D. Vankar, D. K. Avasthi, D. Kabiraj, and G. K. Mehta, Thin Solid Films **305**, 88 (1997).
[21]A. Dunlop, G. Jaskierowicz, P. M. Ossi, and S. Della-Negra, Phys. Rev. B **76**, 155403 (2007).
[22]P. T. Pandey, G. L. Sharma, D. K. Awasthi, and V. D. Vankar, Vacuum **72**, 297 (2003).
[23]P. M. Koinkar, R. S. Khairnar, S. A. Khan, R. P. Gupta, D. K. Avasthi, and M. A. More, Nucl. Instrum. Methods Phys. Res. B **244**, 217 (2006).
[24]J. F. Ziegler, J. P. Biersack, and U. Littmark, *The Stopping and Ranges of Ions in Solids* (Pergamon, New York, 1985).
[25]Z. Sun, J. R. Shi, B. K. Tay, and S. P. Lau, Diamond Relat. Mater. **9**, 1979 (2000).
[26]A. C. Ferrari and J. Robertson, Phys. Rev. B **63**, 121405 (2001).
[27]J. Michler, Y. von Kaenel, J. Stiegler, and E. Blank, J. Appl. Phys. **83**, 187 (1998).
[28]A. C. Ferrari and J. Robertson, Phys. Rev. B **61**, 14095 (2000).
[29]L. Fayette, B. Marcus, M. Mermoux, G. Tourillon, K. Laffon, P. Parent, and F. Le Normand, Phys. Rev. B **57**, 14123 (1998).
[30]L. Ponsonnet, C. Donnet, K. Varlot, J. M. Martin, A. Grill, and V. Patel, Thin Solid Films **319**, 97 (1998).
[31]D. S. Grierson, A. V. Sumant, A. R. Konicek, M. Abrecht, J. Birrell, O. Auciello, J. A. Carlisle, T. W. Scharf, M. T. Dugger, P. U. P. A. Gilbert, and R. W. Carpick, J. Vac. Sci. Technol. B **25**, 1700 (2007).
[32]J. F. Morar, F. J. Himpsel, G. Hollinger, J. L. Jordon, G. Hughes, and F. R. McFeely, Phys. Rev. B **33**, 1346 (1986).
[33]L. J. Huang, I. Bello, W. M. Lau, S.-T. Lee, P. A. Stevens, and B. D. DeVries, J. Appl. Phys. **76**, 7483 (1994).
[34]J. Birrell, J. E. Gerbi, O. Auciello, J. M. Gibson, D. M. Gruen, and J. A. Carlisle, J. Appl. Phys. **93**, 5606 (2003).
[35]M. Lűbbe, P. R. Bressler, D. Drews, W. Braun, and D. R. T. Zahn, Diamond Relat. Mater. **7**, 247 (1998).
[36]G. Comelli, J. Stöhr, C. J. Robinson, and W. Jark, Phys. Rev. B **38**, 7511 (1988).
[37]R. Gago, M. Vinnichenko, H. U. Jäger, A. Yu. Belov, I. Jiménez, N. Huang, H. Sun, and M. F. Maitz, Phys. Rev. B **72**, 014120 (2005).
[38]H.-K. Jeong, H.-J. Noh, J.-Y. Kim, M. H. Jin, C. Y. Park, and Y. H. Lee, Europhys. Lett. **82**, 67004 (2008).
[39]A. Laikhtman, I. Gouzman, and A. Hoffman, Diamond Relat. Mater. **9**, 1026 (2000).
[40]R. Gago, I. Jiménez, and J. M. Albella, Surf. Sci. **482–485**, 530 (2001).
[41]I. Gouzman and A. Hoffman, Diamond Relat. Mater. **9**, 378 (2000).
[42]P. Kovarik, E. B. D. Bourdon, and R. H. Prince, Phys. Rev. B **48**, 12123 (1993).
[43]S. Prawer, J. L. Peng, J. O. Orwa, J. C. McCallum, D. N. Jamieson, and L. A. Bursill, Phys. Rev. B **62**, R16360 (2000).
[44]H. C. Chen, private communication (2013).
[45]M. Jaouen, G. Tourillon, J. Delafond, N. Junqua, and G. Hug, Diamond Relat. Mater. **4**, 200 (1995).
[46]A. V. Sumant, D. S. Grierson, J. E. Gerbi, J. A. Carlisle, O. Auciello, and R. W. Carpick, Phys. Rev. B **76**, 235429 (2007).
[47]J.-Y. Raty, G. Galli, C. Bostedt, T. W. van Buuren, and L. J. Terminello, Phys. Rev. Lett. **90**, 037401 (2003).
[48]E. Rohrer, C. F. O. Graeff, R. Janssen, C. E. Nebel, M. Stutzmann, H. Güttler, and R. Zachai, Phys. Rev. B **54**, 7874 (1996).